Radiation Measurements 148 (2021) 106661

Contents lists available at ScienceDirect

Radiation Measurements

journal homepage: www.elsevier.com/locate/radmeas

Monte Carlo calculation of organ dose coefficients for internal dosimetry: Results of an international intercomparison exercise

Maria Zankl [a,*], José-María Gómez Ros [b], Montserrat Moraleda [b], Uwe Reichelt [c], Deepak K. Akar [d,e], Jorge Borbinha [f], Laurent Desorgher [g], Salvatore Di Maria [f], Jaafar EL Bakkali [h], Karin Fantinova [i], Paolo Ferrari [j], Sebastian Gossio [k], John Hunt [l], Zoran Jovanovic [m], Han Sung Kim [n], Dragana Krstic [m], Yi-Kang Lee [o], Minal Y. Nadar [d], Dragoslav Nikezic [m], Hemant K. Patni [d], Manohari Murugan [p], Sebastian Triviño [q]

[a] Helmholtz Zentrum München (GmbH) German Research Center for Environmental Health, Institute of Radiation Medicine, Ingolstädter Landstr. 1, 85764, Neuherberg, Germany
[b] CIEMAT – Centro de Investigaciones Energéticas, Medioambientales y Tecnológicas, Madrid, Spain
[c] Technical University Dresden, Dresden, Germany
[d] Bhabha Atomic Research Centre, Mumbai, India
[e] Homi Bhabha National Institute, Mumbai, India
[f] Centro de Ciências e Tecnologias Nucleares, Instituto Superior Técnico – Universidade de Lisboa, Lisboa, Portugal
[g] Institute of Radiation Physics IRA, Lausanne University Hospital and University of Lausanne, CH-1007, Lausanne, Switzerland
[h] Nuclear Medicine Department, Military Hospital Mohammed V, Rabat, Morocco
[i] SURO National Radiation Protection Institute, Prague, Czech Republic
[j] ENEA - Radiation Protection Institute, Bologna, Italy
[k] Autoridad Regulatoria Nuclear, Buenos Aires, Argentina
[l] Instituto de Radioproteção e Dosimetria/CNEN, Rio de Janeiro, Brazil
[m] University of Kragujevac, Faculty of Science, Kragujevac, Serbia
[n] Korea Institute of Radiological and Medical Sciences KIRAMS, Seoul, South Korea
[o] Université Paris-Saclay, CEA Service d'Études des Réacteurs et de Mathématiques Appliquées, 91191, Gif sur Yvette, France
[p] Indira Gandhi Centre for Atomic Research, Kalpakkam, India
[q] CNEA, Comisión Nacional de Energía Atómica, Buenos Aires, Argentina

ARTICLE INFO

Keywords:
Intercomparison exercise
Monte Carlo
Reference phantoms
Internal dosimetry

ABSTRACT

EURADOS Working Group 6 has organized an intercomparison exercise on the use of the ICRP Reference Computational Phantoms with radiation transport codes. This paper summarizes the results of a specific task from the intercomparison exercise modelling internal radiation sources. The quantities to be calculated were absorbed fractions and specific absorbed fractions for monoenergetic photon and electron sources as well as S-values for two radionuclides in four source organs. Twelve participants from eleven countries participated in this specific task using the Monte Carlo radiation transport codes FLUKA, Geant4, the MCNP code family, PenEasy, TRIPOLI-4 and VMC. Although some participants provided initial solutions in good agreement with the master solution evaluated by the organizers, differences of factors or even orders of magnitude were also found. Following feedback from the organizer, most participants submitted revised solutions that were mostly in better agreement with the master solution, although this was not always the case. Some initial and revised results are discussed in detail in this paper, and the reasons of mistakes are described as far as they were revealed by the participants. A full account of all results is presented in specific annexes as supplemental material.

* Corresponding author.
E-mail address: zankl@helmholtz-muenchen.de (M. Zankl).

https://doi.org/10.1016/j.radmeas.2021.106661
Received 15 July 2021; Received in revised form 17 September 2021; Accepted 20 September 2021
Available online 2 October 2021

1. Introduction

Working Group 6 "Computational Dosimetry" of the European Radiation Dosimetry Group (EURADOS) recently organized an intercomparison study on the usage of the adult reference computational phantoms (ICRP, 2009) issued jointly by the International Commission on Radiological Protection (ICRP) and the International Commission on Radiation Units and Measurements (ICRU). Various exercises of practical interest in occupational, environmental or medical dosimetry were defined. Participants were invited to attempt to solve the tasks and submit results to the organizers which were then compared against the organizers' master solutions. Besides testing how well the phantoms have been implemented by the participants in their models, further aims of the intercomparison exercise were to provide an opportunity for the participants to improve their computational procedures via feedback, to identify common pitfalls, and to gain insight into the status of voxel phantom usage in computational dosimetry.

The current paper focusses on one of the exercises dealing with internal radiation sources inside specific organs of the male and female reference computational phantoms. The sources considered were monoenergetic photons and electrons, and two radionuclides. The specification of the task is described in detail, and the history of submitted solutions including feedback between the organizers and the participants and the final submitted solutions is summarized.

2. Problem set-up

The aims of this task of the intercomparison exercise were to evaluate (1) absorbed fractions (AF) and specific absorbed fractions (SAF) of energy in specified "target" organs for (1a) monoenergetic photons and (1b) monoenergetic electrons emitted in specific "source" organs of both phantoms, and (2) S-values for the same source and target organ combinations for specific radionuclides.

The Absorbed Fraction, AF, is the fraction of radiation energy E_i emitted within the source tissue r_S at time t that is absorbed in the target tissue r_T (Bolch et al., 2009); this is a dimension-less quantity. The symbol is $\varphi(r_T \leftarrow r_S, E_i, t)$. The target organ under consideration can be the same as the source organ – this case is often referred to as "self-absorption" or "self-irradiation", or the source and target organs are different, often termed as "cross-irradiation" or "cross-fire". For weakly penetrating radiation, such as electrons or low-energy photons, most of the energy is absorbed close to where it is released,i.e., mainly in the source organ itself, and consequently the self-absorption AFs are close to unity, whereas only a small amount of the released energy has the potential to leave the source organ and irradiate more distant organs in the body, and hence the cross-fire AFs are much lower, often close to zero. The Specific Absorbed Fractions, SAF, $\Phi(r_T \leftarrow r_S, E_i, t)$, are Absorbed Fractions divided by the target organ mass, with the unit kg^{-1}.

$$\Phi(r_T \leftarrow r_S, E_i, t) = \frac{\varphi(r_T \leftarrow r_S, E_i, t)}{M(r_T, t)} \quad (1)$$

Both AF and SAF are evaluated for monoenergetic radiations. The S-value is specific to a radionuclide and is given as

$$S(r_T \leftarrow r_S, t) = \frac{1}{M(r_T, t)} \sum_i E_i Y_i \, \varphi(r_T \leftarrow r_S, E_i, t) = \frac{1}{M(r_T, t)} \sum_i \Delta_i \, \varphi(r_T \leftarrow r_S, E_i, t) \quad (2)$$

where E_i is the mean (or individual) energy of the i^{th} nuclear transition, Y_i is the number of i^{th} nuclear transitions per nuclear transformation, and Δ_i is their product (i.e., the total energy of the i^{th} transition per nuclear transformation). The S-value is the absorbed dose rate in the target organ per unit activity of the energy released in the source organ (in Gy $(Bq\ s)^{-1}$).

Source organs in this exercise were: liver, thyroid, stomach contents (St-cont) and urinary bladder contents (UB-cont), and the target regions were: liver, thyroid, stomach wall (St-wall), urinary bladder wall (UB-wall), lungs, and red bone marrow (R-marrow). The source organs were selected due to their frequent practical relevance as source organs for nuclear medicine and nuclear accident dosimetry application: the stomach is part of the intake path in case of radionuclide ingestion, the liver is an important detoxing organ, the urinary bladder is part of the excretion pathway, and the thyroid would accumulate specific radionuclides such as iodine. The target organs are a selection of those organs known to be radiation sensitive and having relatively large tissue weighting factors in the evaluation of effective dose (ICRP, 2007). The radiation emitter should be considered as homogeneously distributed throughout the entire volume of each source organ separately. The energies to be considered for the monoenergetic photons and electrons were: 0.01, 0.05, 0.1, 0.2, 0.5, 1.0, and 3.0 MeV; and the radionuclides to be considered were ^{18}F and ^{99m}Tc routinely used in medical image acquisition in SPECT (Single Photon Emission Computed Tomography) and positron emission tomography (PET). The decay data were taken from ICRP Publication 107 (ICRP, 2008) and given in annexes of the intercomparison specification in tabular form. For the two radionuclides, S-values should be evaluated.

The reference computational phantoms should be used as described in ICRP Publication 110 (ICRP, 2009) with the organ and tissue masses given there. In contrast to the specific absorbed fractions of ICRP Publication 133 (ICRP, 2016), separate blood content should not be added to the organ and tissue masses. An exception are the lungs which comprise the following organ identification numbers: 96 (left lung, blood), 97 (left lung, tissue), 98 (right lung, blood), and 99 (right lung, tissue). This definition follows Annexes C and D of ICRP Publication 110. For red bone marrow and endosteum (earlier called "bone surface") dosimetry, the method proposed in ICRP Publication 116 (ICRP, 2010) was recommended; i.e., usage of dose response functions or dose enhancement factors in case of photons/gammas. The bone dosimetry method should be stated explicitly, and any bone dosimetry method deviating from ICRP Publication 116 should be explained in detail.

A Microsoft Excel template was provided for entering the participants' solutions in a pre-defined format in order to ease evaluation by the responsible person. The template contained also a general part asking for personal and affiliation details, as well as information about the transport code used and its version, the cross-section libraries, cut-off values chosen, the potential use of kerma approximation, and the method of bone dosimetry applied.

Before the task specifications for the intercomparison exercise were distributed, a so-called "master solution" of the present task was calculated by the main organizer of the task. A second solution was provided by several of the co-organizers. Unfortunately, the co-organizers were not able to provide a full solution for all aspects of the task, which was indeed the most extensive one of the entire intercomparison exercise. Luckily, those absorbed fraction and specific absorbed fraction data (Zankl et al., 2012) were available to the organizer that had been calculated for ICRP Publication 133 (ICRP, 2016) using the original phantom organ masses of ICRP Publication 110 (ICRP, 2009). For the final version of ICRP Publication 133, subsequent corrections were applied to these primary data to account for organ masses including also local blood volume in addition to the parenchyma masses (ICRP, 2016). Since the original phantom organ masses of ICRP Publication 110 should be used for the present study, these original ICRP data were used as back-up for the master solution. Since agreement of the master solution with these previous data and those provided by the co-organizers could be established within acceptable limits (mostly within a few percent), they were used as the reference, against which the participants' results were compared.

3. Initial results

Twelve participants (or groups of participants) from eleven countries (Argentina, Brazil, Czech Republic, France, India, Italy, Morocco,

Portugal, South Korea, Serbia and Switzerland) submitted solutions for this task; in some cases, several researchers teamed up, shared the work among them and submitted a common solution together. Only one participant submitted a whole solution treating all aspects of the task; mostly only partial solutions were provided, treating only one phantom or treating only photons, and mostly omitting treatment of the radionuclide S-values.

The following radiation transport codes were used by the participants: FLUKA (Battistoni et al., 2006), Geant4 (Agostinelli et al., 2003) (2 participants), MCNP (Briesmeister, 1986; Werner et al., 2017) (4 p.), MCNPX (Pelowitz, 2008) (2 p.), PenEasy (Sempau et al., 2011), TRIPOLI-4 (Brun et al., 2015), and VMC (Hunt et al., 2004). A detailed summary of the transport codes used, the cross-section libraries, cutoff values chosen, and the potential use of kerma approximation is given in Table 1.

The different methods of bone dosimetry are presented and discussed in more detail in a separate paper of this Special Issue (Zankl et al., 2021b). In principle, two different methods should be used in the context of this exercise for evaluating the dose to the red bone marrow. For photons and gammas, the ICRP recommends the use of so-called fluence-to-dose response functions (see Annex D of ICRP Publication 116 (ICRP, 2010)), and for electrons and betas, it is recommended to evaluate a mass-weighted average spongiosa dose as estimate of red bone marrow dose. Two participants (d and k) did not evaluate red bone marrow doses at all, five (a, b, e, f and h) used fluence-to-dose response functions or dose enhancement factors for their photon simulations, two (c and j) used mass-averaged spongiosa doses as surrogate for red bone marrow doses also for photons, one participant (l) used a "homemade" method which was not further specified, and two (g and i) indicated "ICRP 116" without specifying exactly which one of the two possibilities they used. In these latter cases, it can be assumed that the mass-weighting method was applied also for the photon calculations.

The master solution was calculated with the radiation transport program package EGSnrc (Kawrakow et al., 2009); the photon cross-section library was an updated version (Seuntjens et al., 2002) of the XCOM database (Berger and Hubbell, 1987), and the cutoff value for photons was 2 keV; for electrons, Bremsstrahlung cross sections from the National Institute of Standards and Technology (NIST) database (Seltzer and Berger, 1985, 1986) were used, and the transport history of electrons was generally terminated when their kinetic energy fell below 20 keV, except for electrons with an initial kinetic energy below 50 keV, whose histories were followed down to 2 keV. The "three-factor method" as described in ICRP Publication 116 (ICRP, 2010), Annex D, was used for bone marrow dosimetry for photons and gammas. This method is equivalent to using fluence-to-dose response functions, and the R-marrow target evaluated thus is identified as "R-marrow (DRF)" in the following. A mass-weighted dose to spongiosa as described in Chapter 3 of ICRP Publication 116 was evaluated as well for these radiations, in order to compare this additional evaluation against the results of the participants who have used this method. This mass-weighted spongiosa dose is identified as "R-marrow (wtd)".

Table 1
Monte Carlo radiation transport codes, cross-section libraries, and cutoff values used in the "Internal dosimetry" task.

MC code and version	Photon cross-section library	Photon cutoff energy or range	Electron cross-section library	Electron cutoff energy or range	Kerma approximation
FLUKA	EPDL97	4 keV	Seltzer and Berger (1986)	5 keV	no
Geant4 10.4	Geant4 standard	1 keV	Geant4 standard	1 keV or 0.5 mm	no
Geant4 10.03	Geant4 standard	0.4274 mm	Geant4 standard	0.004274 mm	no
MCNP4C3	mcplib84	1 keV	el03	1 keV	yes
MCNP	not given	1 keV	not given	1 keV	no
MCNP 6.1	not given	10 keV	not given	10 keV	no
MCNP 6.2	mcplib84	1 keV	el03	1 keV	no
MCNPX	mcplib84	1 keV	el03	1 keV	no
MCNPX 2.6.0	mcplib84	1 keV	el03	1 keV	?
PenEasy	EDPL 97 cross section library	1 keV	Seltzer and Berger (1986)	1 keV	no
TRIPOLI-4	ENDL97	1 keV	EEDL + Bremsstrahlung	1 keV	no
VMC	NIST XCOM	10 keV	n.a.	n.a.	yes

For the master solution of the S-values, energies for individual particle histories were sampled from the decay spectra according to their relative yields, thus avoiding the necessity of interpolating the monoenergetic SAF values.

For each source organ, 9×10^8 histories were simulated for every photon and electron energy as well as for every radionuclide. For photons and source and target organ combinations that are not too distant, this resulted in coefficients of variation generally well below 1%, often below 0.1%, but for low energies and distant organ pairs, such as thyroid and urinary bladder, the coefficient of variation amounts up to several tens of percent. For electrons, the coefficients of variation are below 1%–5% only for target organs that are either large or quite close to the source organ. For distant organ pairs and small target organs, the coefficient of variation amounts up to several tens of percent, especially for low energies.

The master solution Absorbed Fractions, together with their statistical uncertainty, are presented in Supplemental Table A1 to Supplemental Table A4 of Annex A for the male and female reference computational phantom and for photons and electrons, respectively. The Specific Absorbed Fractions are not presented, since these are simply derived by dividing the Absorbed Fraction by the target organ mass and show, hence, the same energy dependence as the Absorbed Fractions. Their separate presentation in tables would, thus, unnecessarily increase the amount of data presented. The S-values for both phantoms and ^{18}F and ^{99m}Tc are presented in Supplemental Table A5 to Supplemental Table A8, together with their statistical uncertainties.

For the initial results submitted by the participants, a large range of deviations from the master solutions was observed: some participants' solutions were within 5–10% agreement with the master solution, others differ by several orders of magnitude.

The participants' initial absorbed fractions for photons in the liver of the male reference phantom are shown in Fig. 1 as ratios of the participants' solution to the master solution. It can be seen that the self-absorption AFs are in good agreement with the master solution for most participants, but underestimations up to factors 2 and 5 respectively were also found. Amazingly, the liver self-absorption AF for participant a is approximately a factor 5 lower than the master solution at 0.5 MeV, whereas it is in excellent agreement (within less than 1%) for all other photon energies. For cross-fire AFs, the situation is generally less favourable. Although again the majority of participants submitted solutions close to the master solution, the ranges of under- and overestimations were larger. The maximum deviations were an underestimation by a factor of 80 for the urinary bladder wall at 0.5 MeV and an overestimation by approximately a factor of 7000 at 0.05 MeV for the thyroid.

Only a small selection of the participants' initial results is shown below. A comprehensive compilation of the results can be found in Annex B of the supplemental material, Supplemental Figure B1 to Supplemental Figure B21. All results are shown in the form of ratios of the participants' solutions to the master solution.

The participants' initial absorbed fractions for photons in the thyroid of the male reference phantom are shown in Supplemental Figure B1. While a majority of the ratios is close to unity for all target organs, there are again large deviations to be seen as well. The largest deviations were an underestimation by a factor of 1446 at 0.01 MeV for thyroid self-

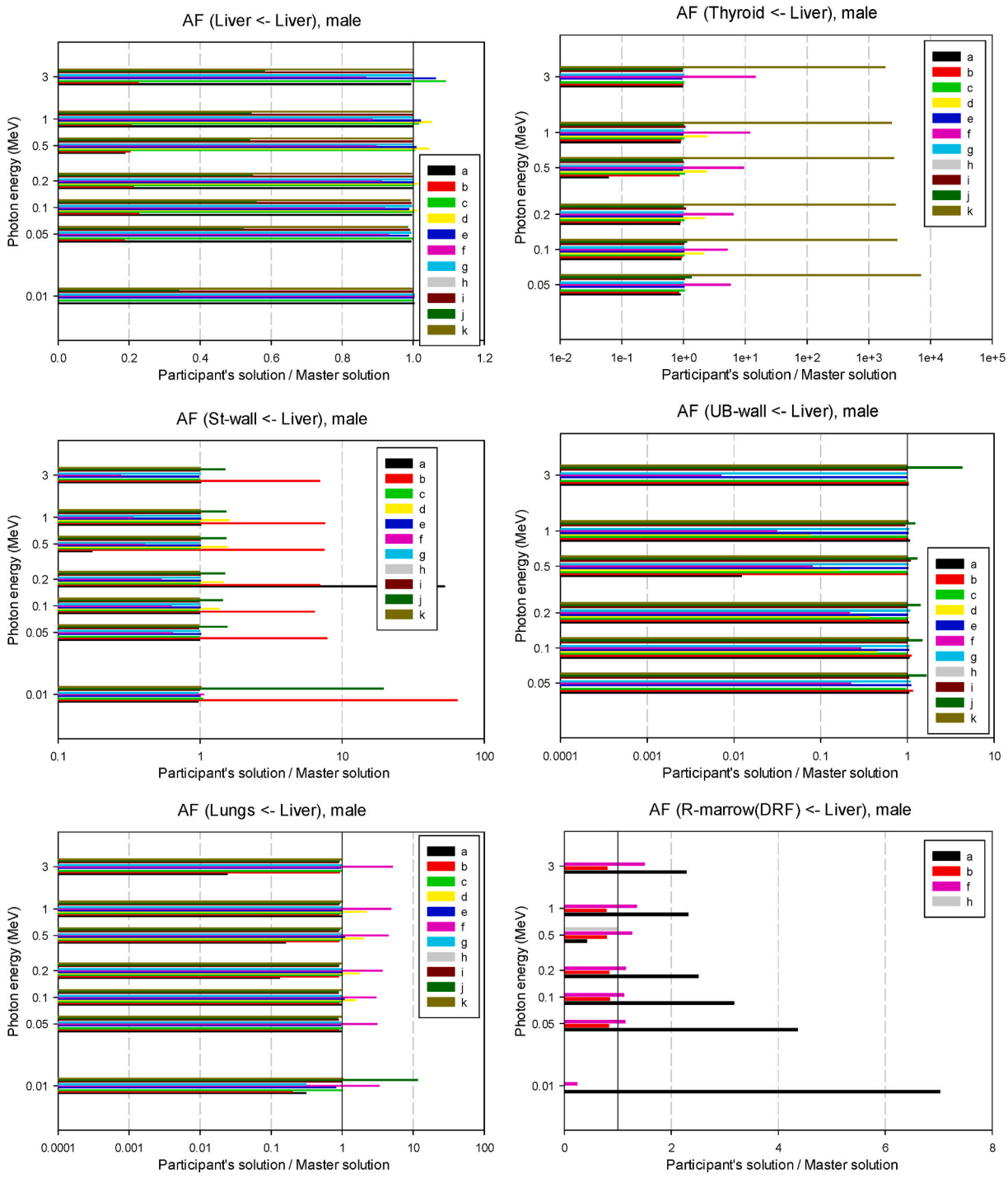

Fig. 1. Ratios of the participants' initial solutions to the master solution for photon sources in the liver of the male reference phantom.

absorption and an overestimation by approx. a factor 137 at 0.05 MeV for the urinary bladder wall.

The participants' initial absorbed fractions for photons in the stomach contents of the male reference phantom are shown in Supplemental Figure B2. Although a majority of the ratios is close to unity for all target organs, large deviations occurred as well. The maximum underestimation was seen for the stomach wall target and amounted to approx. a factor of 290, whereas the maximum overestimation was for the urinary bladder wall at 0.05 MeV and amounted to a factor of approx. 5300.

For photons in the urinary bladder contents of the male reference phantom, the results are shown in Supplemental Figure B3. The largest underestimation was seen for the urinary bladder wall target and amounted to approx. a factor of 2500, whereas the largest overestimation occurred for the thyroid target and amounted approx. to a factor of 12,350. It should be noted, however, that the master solution for the thyroid target shows a very low value on the one hand and a large statistical uncertainty on the other hand; large deviations of the participants' solution are, hence, to be expected and should not be interpreted as indicating problems in the participants' calculation methods.

For red bone marrow as target, a further set of ratios is shown; since three participants used mass-weighted spongiosa AFs to estimate red bone marrow AFs, these results are compared against an additional master solution using the same approach. These data are shown in Fig. 2 for all source organs. For the liver source, the deviations ranged from an

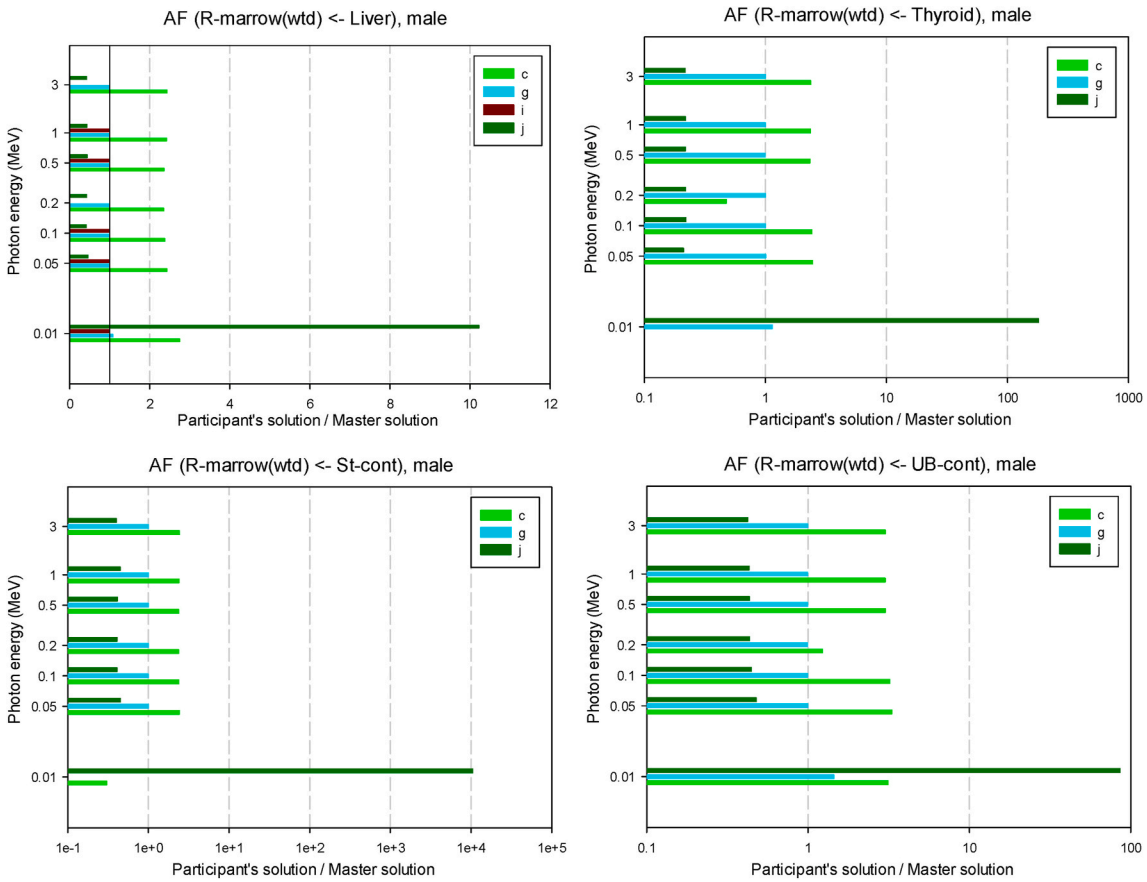

Fig. 2. Ratios of the participants' initial red bone marrow AFs to the master solution evaluated as mass-weighted spongiosa AF for photon sources in various organs of the male reference phantom. (For interpretation of the references to colour in this figure legend, the reader is referred to the Web version of this article.)

underestimation by approx. a factor of 70 at 3 MeV to an overestimation by approx. a factor of 10 at 0.01 MeV. For the thyroid source, the maximum underestimation was approx. a factor of 5 for energies from 0.05 MeV to 3 MeV, and the maximum overestimation was by approx. a factor of 180 at 0.01 MeV. For the source in stomach contents, the maximum overestimation amounted approx. to a factor of 10,500 at 0.01 MeV, and for the urinary bladder content source the maximum overestimation was by approx. a factor 85 at 0.01 MeV.

The participants' initial results for photon sources in the female phantom are shown in Supplemental Figure B4 to Supplemental Figure B8 and exhibit a similar behaviour with many ratios being close to unity on the one hand and the occurrence of large under- and overestimations in single cases, by factors or even orders of magnitude, on the other hand.

The participants' initial results for electron sources in the male phantom are shown in Fig. 3 for the liver source and for the other source organs in Supplemental Figure B9 to Supplemental Figure B11 and for the female in Supplemental Figure B12 to Supplemental Figure B15. It can be seen that fewer participants provided solutions for electrons than for photons. The AFs for red bone marrow for the master solution were evaluated as mass-weighted average of the spongiosa AFs in individual bones, as recommended for electrons in ICRP Publication 116 (ICRP, 2010).

Electrons are weakly penetrating, especially those with lower energies. Hence, cross-fire AFs are bound to be small, especially when the source and target organs are distant from each other, such as the urinary bladder and the thyroid. As can be seen from Supplemental Table A3 and Supplemental Table A4, the master solution has large statistical uncertainties for these cases, and this was also the case for the participants' solutions. Hence, it is not surprising and fully acceptable that there is lower agreement between the participants' solutions and the master solution for electrons. The observed deviations are, however, sometimes larger than what could be expected. This is especially true for self-absorption AFs and irradiation of the stomach and urinary bladder walls by their respective contents. Especially for these latter situations, the deviations found which amount to several orders of magnitude in some cases, are too large to be explained by statistical uncertainties.

The specific absorbed fractions showed the same relations to the master solution as the absorbed fractions in most cases. For some participants, the SAFs of single target organs behaved differently than the AFs, indicating that the masses of these organs deviated from those of the reference phantoms. For one participant, the male organ doses seemed to differ from those of the reference phantom, whereas those for the female phantom were obviously in agreement. The most interesting exception was found for one participant, where the ratio of AF and SAF for the bone marrow was energy-dependent instead of the constant factor expected due to dividing the AF by the organ mass for evaluating the SAF.

Supplemental Figure B16 and Fig. 4 show the S-values for the male and female reference phantom for ^{18}F, respectively. Since ^{18}F is a positron emitter, the red bone marrow S-values have been evaluated as mass-weighted average S-values of the individual spongiosa regions.

It can be seen that many participants' solutions agree with the master solutions within approx. 10–20%, but there are also many larger deviations. For the male phantom, the largest underestimation occurred for S(St-wall←St-cont) and was approx. a factor of 100, and the largest overestimation of approx. a factor 6500 was for S(Thyroid←St-cont). For the female phantom, the maximum under- and overestimations were for the same organ pairs and amounted to factors of approx. 140 and 10,000, respectively.

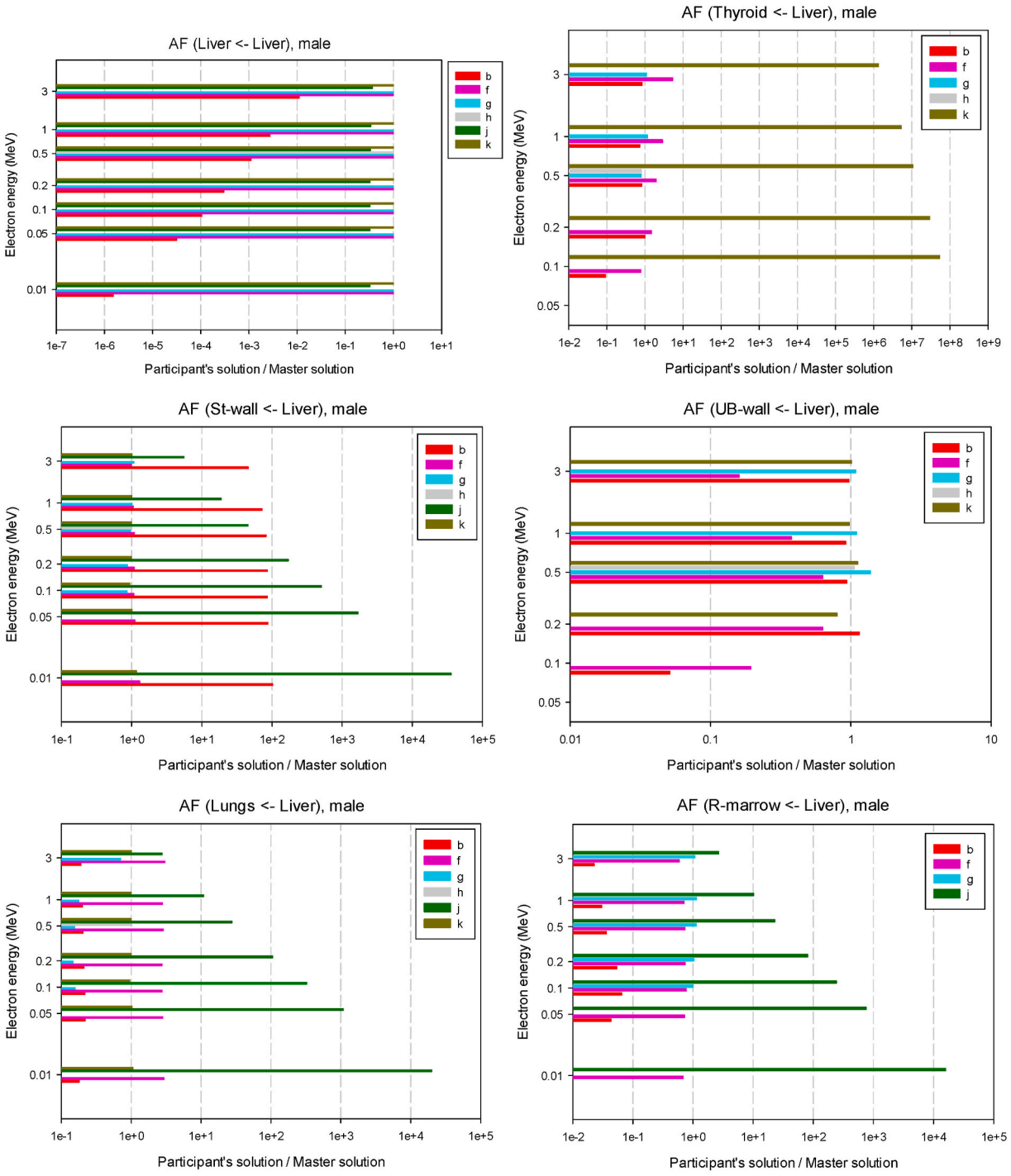

Fig. 3. Ratios of the participants' initial solutions to the master solution for electron sources in the liver of the male reference phantom.

The S-values for ^{99m}Tc have two components – one from photons, the other from electrons. The S-value contributions from gammas/photons, betas/electrons and the sum of both are shown in Supplemental Figure B17 to Supplemental Figure B19 for the male and in Fig. 5, Supplemental Figure B20 and Supplemental Figure B21 for the female reference phantom. For the photon/gammas, again two versions of red bone marrow S-values have been evaluated as master solution: "R-marrow (DRF)" applying fluence-to-dose response functions or dose enhancement factors; "R-marrow (wtd)" as mass-weighted average of the S-values for the individual spongiosa regions. The latter was evaluated to provide a possibility to compare it against the solutions of those participants who used that method. For the electron/beta contribution, only the latter method was applied, since this is appropriate for electrons (ICRP, 2010). Of course, those participants applying the kerma approximation in their simulation did not provide an electron contribution to the S-values for ^{99m}Tc. For these participants, total ^{99m}Tc S-values could not be evaluated. For the total S-values, the photon and electron contributions have been summed up, and hence again two versions of master S-values for the red bone marrow are included. For photons, the largest underestimations were by approx. a factor 10, and overestimations ranged approximately up to a factor of 2.4; for electrons, the largest over- and underestimations were by orders of magnitude. As can be seen from Supplemental Table A7 and Supplemental Table A8, the master solution again has large statistical uncertainties for

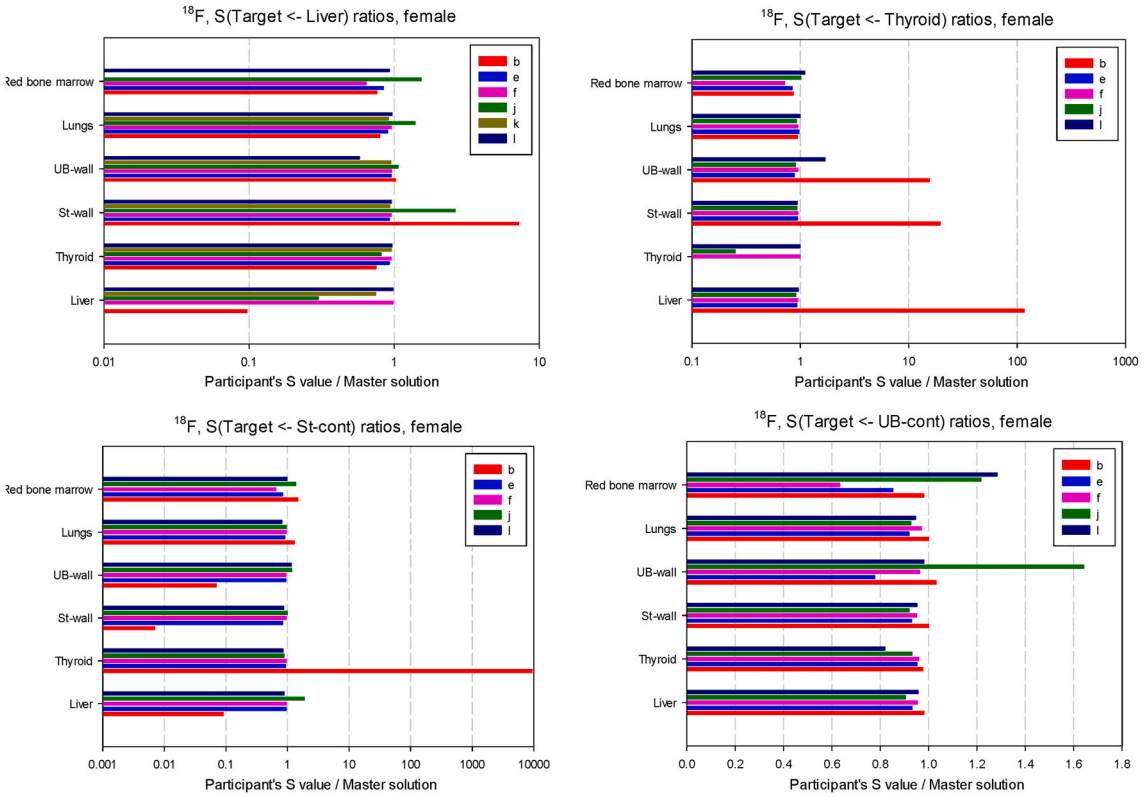

Fig. 4. Ratios of the participants' initial solutions to the master solution for the radionuclide ^{18}F for the female reference phantom.

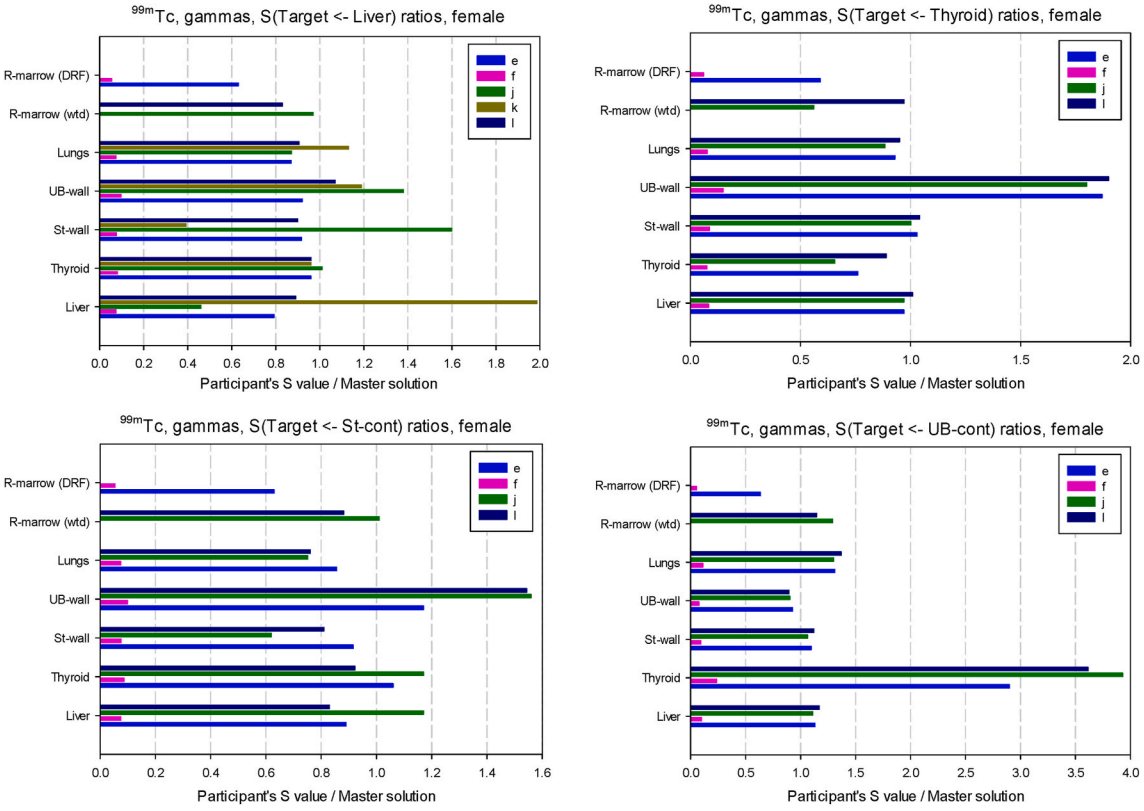

Fig. 5. Ratios of the participants' initial solutions to the master solution for the radionuclide ^{99m}Tc (photon contribution) for the female reference phantom.

some distant organ pairs, and this was also the case for the participants' solutions. Hence, it is not surprising and fully acceptable that there is low agreement of the participants' solutions with the master solution for the electron/beta contribution, especially for distant organ pairs. These over- and underestimations might be artificial and should not be overrated.

4. Revision of results

4.1. First feedback

All participants were informed how their results compared to the master solution. The following is one specific example of the first feedback to one of the participants:

"Your solutions show generally excellent agreement with the master solution, except some specific cases:

- Red bone marrow AFs differ substantially from the master solution.
- SAFs for red bone marrow are not related to AFs by a constant factor (i.e., target tissue mass).
- For the male reference phantom, there are several problems:
  - o the values for 0.5 MeV are generally much too low
  - o for liver source and lung target, several values are much too low (except 0.05 MeV, 0.1 MeV, 1 MeV)
  - o for UB-cont source, most AF and SAF values are much too high, except for target UB-wall, where they are much too low. For this source, only the R-marrow AFs are closer to the master solution

Could you please verify your.

- method of evaluating the red bone marrow AFs and SAFs,
- red bone marrow masses, and
- urinary bladder content source in the male phantom?"

4.2. Reports by participants of reasons for erroneous first/second results

The errors that were detected by the participants upon first feedback were the following: One participant had mis-arranged his results in the template provided for filling in the results. Upon correct arrangement, they turned out to agree within a few percent with the master solution. For two participants, the lung masses did not agree with the reference phantoms. It turned out that only the lung tissue had been considered without including the blood vessels in the lungs. (The lungs are the only organ for which also blood content should be considered, as described in Annex C of ICRP Publication 110.) One participant used the organ masses of ICRP Publication 133 including regional blood content instead those given in ICRP Publication 110 which leads to differences in the SAFs and S-values up to approx. 30%.

A further common source for erroneous initial solutions were typing or copy-paste errors when entering the solutions into the provided template.

Some participants did not explain exactly which method of bone dosimetry they applied and claimed using the method according to "ICRP 116". From the magnitude of the values, it could be concluded that mostly a mass-weighting of spongiosa doses in individual bones was applied.

4.3. Repeated feedback and its results

Most participants used the opportunity of submitting revised results, whereas a few did not. These latter were participants a, f, g, and k. In some cases, there were several rounds of revised solutions and feedback about their relation to the master solution, sometimes – but not always – leading to a gradual improvement of the results. In individual cases, unfortunately, parts of the solutions were worsened during the revision.

Several participants submitted more complete solutions in course of their revisions, since they had not found the time to perform all simulations before the initial deadline, or they improved the statistical quality of their results by simulating larger numbers of histories. Participant j changed the red bone marrow dosimetry method and applied the dose response functions of ICRP Publication 116 for photons for the revised results, and participant l used a user-friendly input, an improved particle tracking method in the geometry package for voxel phantoms (Lee et al., 2021) and an updated bremsstrahlung model for the revision of results.

Unfortunately, however, most participants did not indicate the changes that they introduced into their simulations or evaluations to arrive at the revised solutions, and thus no insights could be gained that might help to give useful hints to participants of potential future intercomparison or teaching actions.

4.4. Summary of revised solutions

The (initial) results of participants a, f, g, and k, who did not submit revised solutions, are not included in the revised set of results, even if they were in parts in acceptable agreement with the master solution.

The revised results for photon sources in the liver of the male phantom are shown in Fig. 6. Again, only a small selection of the participants' revised results is presented here in the article main body, and all other revised results are shown in Annex C of the supplemental material, in the same order as the participants' initial solutions in Annex B.

It can be seen that the AFs for liver self-absorption are in excellent agreement for most participants and agree within approx. 10% for all participants. For cross-fire AFs many of the revised solutions are much closer to the master solution than the original solutions were, but there are still large under- and overestimations. The largest underestimation is by approx. a factor 13 for the urinary bladder wall at 1 MeV, and the largest overestimation is by a factor of 2.4 for the thyroid, also at 1 MeV.

The participants' revised absorbed fractions for photons in the thyroid of the male reference phantom are shown in Supplemental Figure C1. It can be seen that a majority of these ratios is close to unity for all target organs and the number and degree of outliers has been considerably reduced compared to the original results of Supplemental Figure B1. Nevertheless, there are still a few large deviations to be seen as well. The largest deviations were an underestimation by a factor of approx. a factor 10 at 0.1 MeV for the stomach wall and an overestimation by approx. a factor 2 at 0.05 MeV for the urinary bladder wall.

The participants' revised absorbed fractions for photons in the stomach contents of the male reference phantom are shown in Supplemental Figure C2. The clear majority of the ratios is close to unity for all target organs, and only a small number of larger deviations occurred. The maximum underestimation is seen for the lung target and amounts to approx. a factor of 14, whereas there are no significant overestimations any more.

For photons in the urinary bladder contents of the male reference phantom, the results are shown in Supplemental Figure C3. There are nearly no larger significant deviations any more. The larger underestimations are by a factor of two at 0.1 MeV for the stomach wall and by approx. a factor 2.5 for the R-marrow for some energies. Overestimations are found only for the thyroid at 0.05 MeV, but this is owed to the large distance of these organs and the consequently large statistical uncertainties of both participants' and master solutions.

The ratios of the participants' revised results and the master solutions for red bone marrow evaluated as mass-weighted spongiosa AFs are shown in Fig. 7 for all source organs. The results of participant i, who made calculations only for liver source, are in exact agreement with the mass-weighted R-marrow target master solution, but the results of both participants c and l show deviations from the master solutions for all source organs.

The revised results for photon sources in the female phantom are

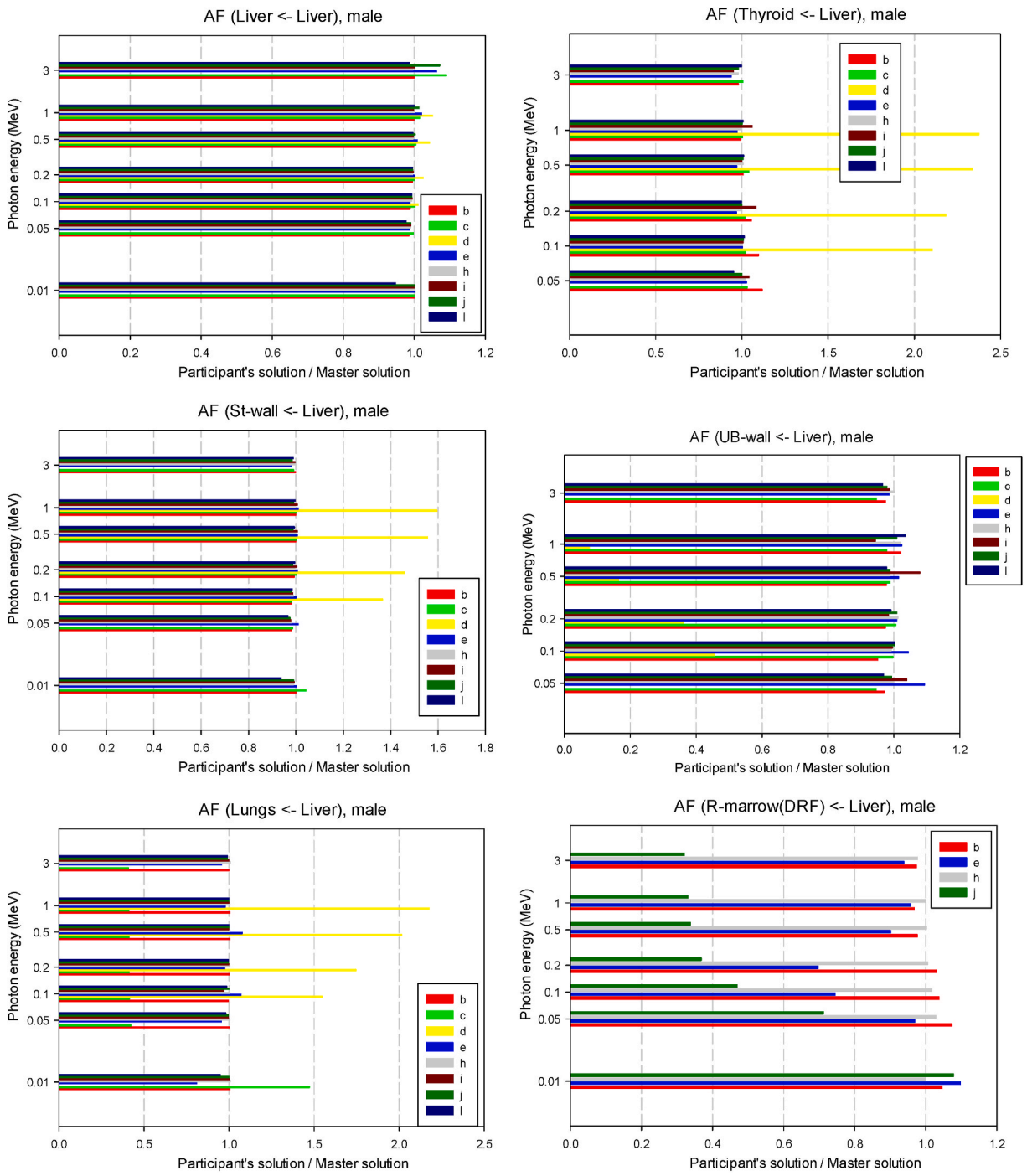

Fig. 6. Ratios of the participants' revised solutions to the master solution for photon sources in the liver of the male reference phantom.

shown in Annex C in Supplemental Figure C4 to Supplemental Figure C8.

The participants' revised results for electron sources in the male phantom are shown in Fig. 8 for the liver source. It can be seen that they are in much better agreement with the master solutions than the original submissions had been. Many results agree with the master solution within only a few percent, and maximum under- and overestimations are in the range of approx. factors 5 (underestimation, for thyroid) and 2 (overestimation, for R-marrow). The participants' revised results for electron sources in all other source organs for the male phantom are shown in Supplemental Figure C9 to Supplemental Figure C11, and for all source organs for the female phantom in Supplemental Figure C12 to Supplemental Figure C15.

Supplemental Figure C16 and Fig. 9 show the S-values for the male and female reference phantom for ^{18}F, respectively. It can be seen again that the revised results are in much better agreement with the master solutions than the original submissions had been. The majority of results agree with the master solution within approx. 20% and often within only a few percent, and maximum underestimations are in the range of approx. factors between 3 and 10 (mostly for R-marrow).

The S-value contributions to ^{99m}Tc from gammas/photons, betas/electrons and the sum of both are shown in Supplemental Figure C17 to Supplemental Figure C19 for the male, and in Fig. 10, Supplemental Figure C20 and Supplemental Figure C21 for the female reference phantom. For the photon/gammas, again two versions of red bone marrow S-values have been evaluated as master solutions: "R-marrow

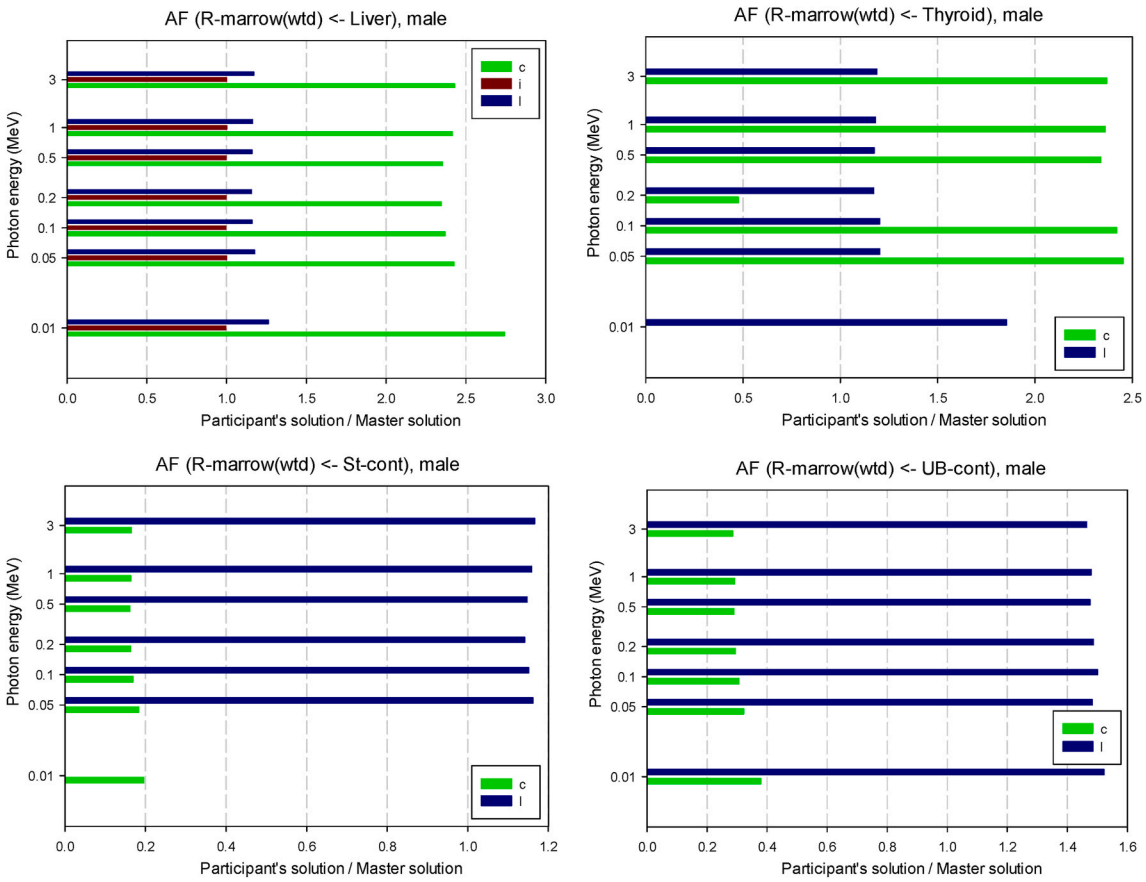

Fig. 7. Ratios of the participants' revised red bone marrow AFs to the master solution evaluated as mass-weighted spongiosa AF for photon sources in various organs of the male reference phantom. (For interpretation of the references to colour in this figure legend, the reader is referred to the Web version of this article.)

(DRF)" and "R-marrow (wtd)". For the total S-values, the photon and electron contributions have been summed up, and hence again two versions of master S-values for the red bone marrow are included. Again, total ^{99m}Tc S-values could not be evaluated for those participants using kerma approximation.

For the photon contribution, the majority of submissions agree with the master solution within approx. 20%–25%, except for cross-fire between thyroid and urinary bladder, where the majority of ratios are close to a factor 2, indicating that the master solution (with statistical uncertainties of 23.5% and 29.5%, respectively) might be too low. More severe outliers are the overestimation by a factor of 5 for S(Liver < - UB-cont) and the underestimations by factors 2 to 4 for the R-marrow target from all source organs. For the beta contribution, the most severe outliers are: (1) overestimations by approx. one order of magnitude for the self-irradiation S-values and the S-values for irradiation of the stomach and urinary bladder walls by these organs' contents and (2) an overestimation by nearly five orders of magnitude for S(Liver < - UB-cont), which is not visible in the figure due to the restricted range of values shown.

5. Discussion

This exercise was probably the most extensive one among the six tasks of the EURADOS Intercomparison Exercise (Zankl et al., 2021a). The number of participants amounting to twelve teams from eleven countries was surprisingly high, and three participants managed even to solve all aspects of this large task, at least as far as the revised solutions are concerned. Most participants, however, could manage only to solve part of the task, e.g., dealing with just one phantom, simulating only photon sources, or not submitting results for the radionuclide S-values.

Several participants were quite successful and provided solutions that were – at least partly – in acceptable agreement with the master solution provided by the organizers of the exercise. On the other hand, one of the more important findings is that in some cases, unfortunately, relatively simple measures of quality assurance have not been applied. For the current exercise, extensive quality assurance could have been made against comparable data that have been published by the ICRP employing the same phantoms with slightly different organ masses (ICRP, 2016). Furthermore, simple plausibility considerations would make clear, for example, that self-absorption AFs can be expected to be much higher than cross-fire AFs, especially for radiations of low penetrability. This is true also for irradiation of walled organs from sources in their contents. Further oddities that might have been detected by plausibility considerations were when the AFs for one single energy were much smaller than those for all other energies considered, or when the SAFs were not showing the same energy dependence as the AFs.

After feedback with the participants, most participants used the opportunity to submit revised results. These were indeed generally in much better agreement with the master solution, although this was not always the case. Some participants revealed the mistakes that they had made with their initial submission. These had several reasons, e.g., misarrangement of the data into the provided template, copy-and-paste or typing errors, or use of organ masses different from those in ICRP Publication 110 (ICRP, 2009). One participant made improvements or refinements to the radiation transport code used, others took the additional time to submit more complete solutions. Unfortunately, several participants did not reveal the measures that they took to improve their results, and thus valuable information was lost that might help other users to avoid the same or similar mistakes. It seems, however, that more fundamental problems with the implementation of the

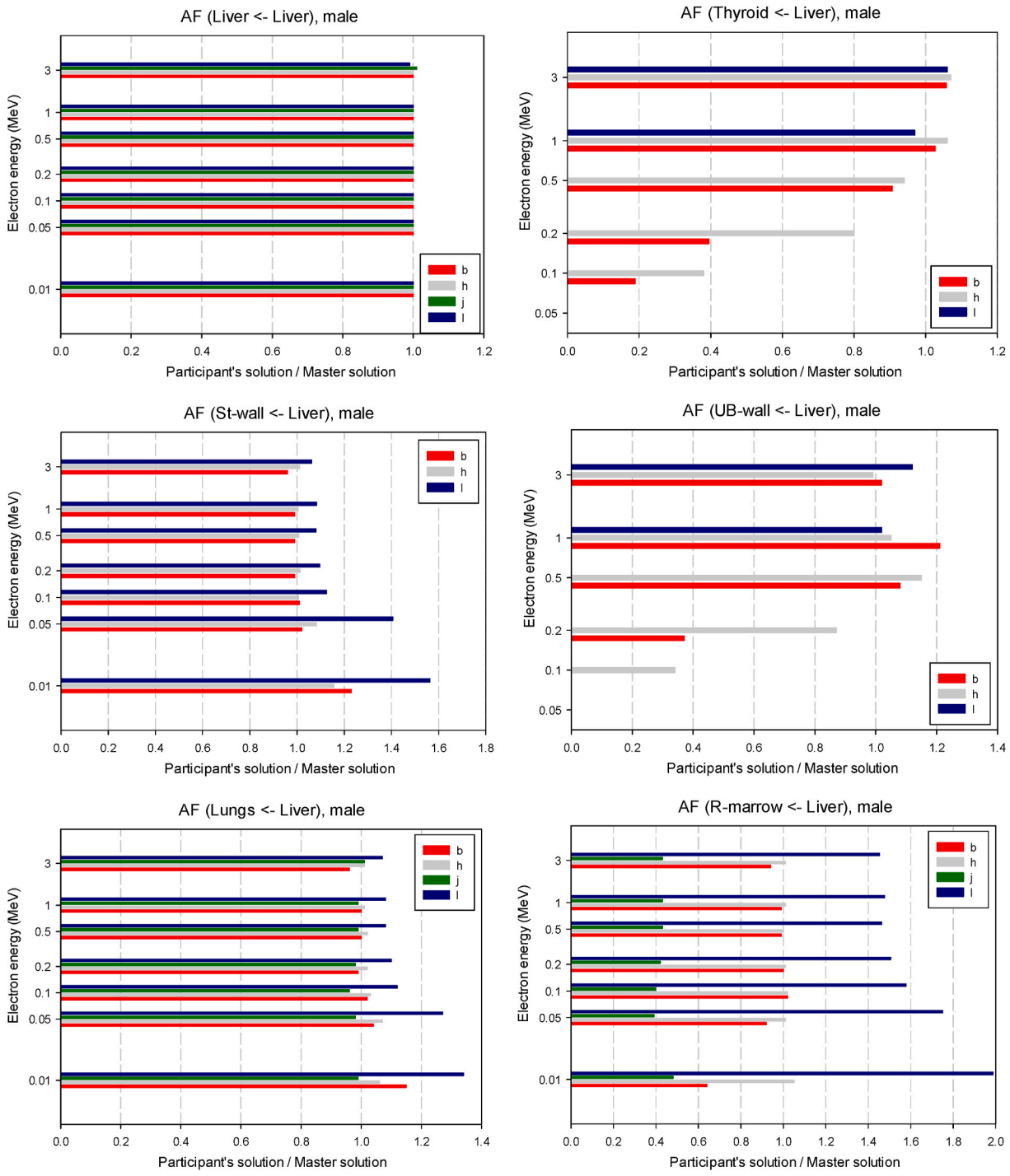

Fig. 8. Ratios of the participants' revised solutions to the master solution for electron sources in the liver of the male reference phantom.

reference phantoms into the Monte Carlo codes have not been encountered.

It was furthermore noted that several participants had difficulties to arrive at correct solutions for the R-marrow coefficients, also for the revised submissions.

6. Conclusions

The Intercomparison Exercise organized by EURADOS WG6 was intended to study the implementation of voxel phantoms in a variety of radiation transport codes. The current task was probably the most extensive one of the entire exercise, and – considering this – the participation by twelve teams from eleven countries was pleasantly high. The Monte Carlo codes used by the participants were FLUKA, Geant4, the MCNP family of codes, PenEasy, TRIPOLI-4, and VMC. Several participants were quite successful and provided solutions that were – at least partly – in acceptable agreement with the master solution provided by the organizers of the exercise. On the other hand, one of the more important findings is that in some cases, unfortunately, measures of quality assurance have not been applied with appropriate carefulness.

Feedback to the participants – sometimes with several feedback loops – helped to find some of the initial mistakes made by individual participants and to improve the results. Unfortunately, not all participants disclosed the changes that they applied to their computational

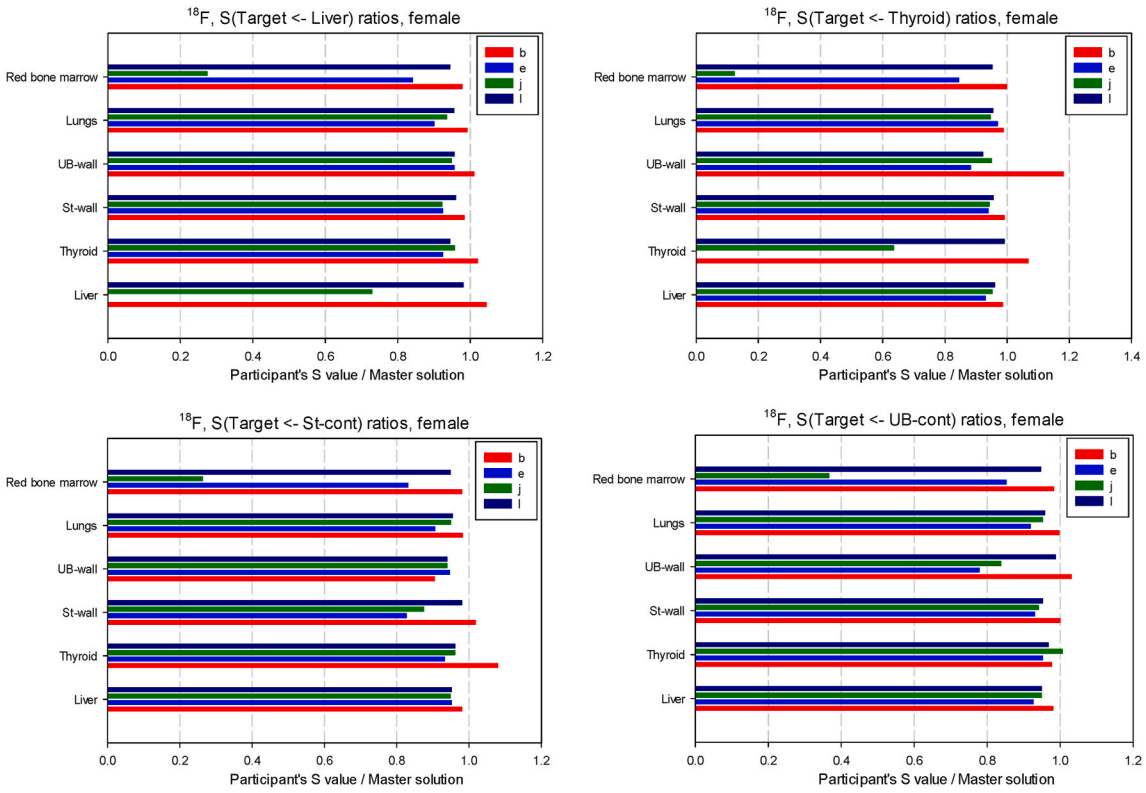

Fig. 9. Ratios of the participants' revised solutions to the master solution for the radionuclide ^{18}F for the female reference phantom.

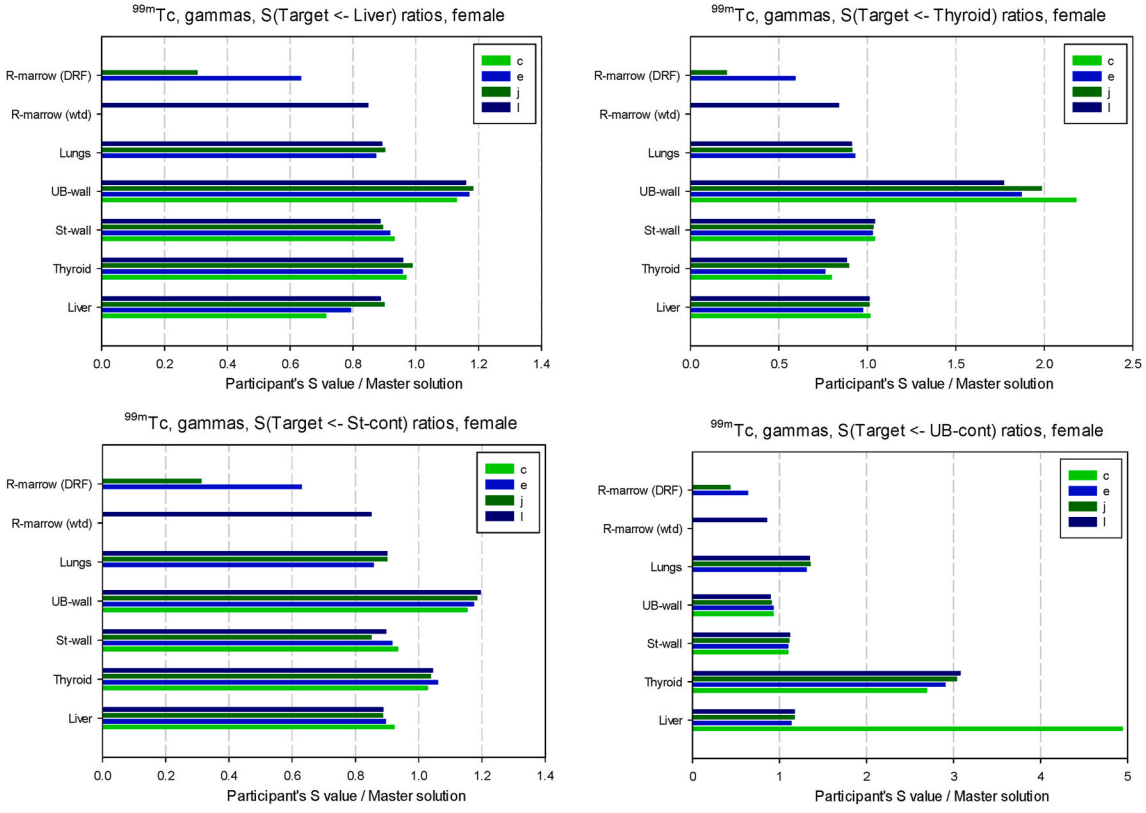

Fig. 10. Ratios of the participants' revised solutions to the master solution for the radionuclide ^{99m}Tc (photon contribution) for the female reference phantom.

procedure in order to arrive at the improved results, and hence sometimes no valuable insights could be gained that could have been communicated also to other participants.

Nevertheless, it has been shown once more that intercomparison exercises are a very valuable tool for establishing good practice in computational dosimetry. On the one hand, they give active users the possibility to benchmark their own results against those of others and against validated master solutions; on the other hand, they provide additional collections of data that may be used for training purposes for future novice users.

Declaration of competing interest

The authors declare that they have no known competing financial interests or personal relationships that could have appeared to influence the work reported in this paper.

Appendix A. Supplementary data

Supplementary data to this article can be found online at https://doi.org/10.1016/j.radmeas.2021.106661.

References

Agostinelli, S., Allison, J., Amako, K., Apostolakis, J., Araujo, H., Arce, P., Asai, M., Axen, D., Banerjee, S., Barrand, G., Behner, F., Bellagamba, L., Boudreau, J., Broglia, L., Brunengo, A., Burkhardt, H., Chauvie, S., Chuma, J., Chytracek, R., Cooperman, G., Cosmo, G., Degtyarenko, P., Dell'Acqua, A., Depaola, G., Dietrich, D., Enami, R., Feliciello, A., Ferguson, C., Fesefeldt, H., Folger, G., Foppiano, F., Forti, A., Garelli, S., Giani, S., Giannitrapani, R., Gibin, D., Gómez Cadenas, J.J., González, I., Gracia Abril, G., Greeniaus, G., Greiner, W., Grichine, V., Grossheim, A., Guatelli, S., Gumplinger, P., Hamatsu, R., Hashimoto, K., Hasui, H., Heikkinen, A., Howard, A., Ivanchenko, V., Johnson, A., Jones, F.W., Kallenbach, J., Kanaya, N., Kawabata, M., Kawabata, Y., Kawaguti, M., Kelner, S., Kent, P., Kimura, A., Kodama, T., Kokoulin, R., Kossov, M., Kurashige, H., Lamanna, E., Lampén, T., Lara, V., Lefebure, V., Lei, F., Liendl, M., Lockman, W., Longo, F., Magni, S., Maire, M., Medernach, E., Minamimoto, K., Mora de Freitas, P., Morita, Y., Murakami, K., Nagamatu, M., Nartallo, R., Nieminen, P., Nishimura, T., Ohtsubo, K., Okamura, M., O'Neale, S., Oohata, Y., Paech, K., Perl, J., Pfeiffer, A., Pia, M.G., Ranjard, F., Rybin, A., Sadilov, S., Di Salvo, E., Santin, G., Sasaki, T., Savvas, N., Sawada, Y., Scherer, S., Sei, S., Sirotenko, V., Smith, D., Starkov, N., Stoecker, H., Sulkimo, J., Takahata, M., Tanaka, S., Tcherniaev, E., Safai Tehrani, E., Tropeano, M., Truscott, P., Uno, H., Urban, L., Urban, P., Verderi, M., Walkden, A., Wander, W., Weber, H., Wellisch, J.P., Wenaus, T., Williams, D.C., Wright, D., Yamada, T., Yoshida, H., Zschiesche, D., 2003. Geant4—a simulation toolkit. Nucl. Instrum. Methods Phys. Res. Sect. A Accel. Spectrom. Detect. Assoc. Equip. 506 (3), 250–303.

Battistoni, G., Muraro, S., Sala, P.R., Cerutti, F., Ferrari, A., Roesler, S., Fasso, A., Ranft, J., 2006. The FLUKA code: description and benchmarking. In: Albrow, M., Raja, R. (Eds.), Hadronic Shower Simulation Workshop. AIP Conference Proceeding, Fermi National Accelerator Laboratory (Fermilab), Batavia, Illinois, pp. 31–49.

Berger, M.J., Hubbell, J.H., 1987. XCOM: Photon Cross Sections on a Personal Computer. National Bureau of Standards (former name of NIST), Gaithersburg, MD.

Bolch, W.E., Eckerman, K.F., Sgouros, G., Thomas, S.R., 2009. MIRD pamphlet No. 21: a generalized schema for radiopharmaceutical dosimetry—standardization of nomenclature. J. Nucl. Med. 50 (3), 477–484.

Briesmeister, J.F., 1986. MCNP - A General Monte Carlo Code for Neutron and Photon Transport, Version 3A. Los Alamos National Laboratory, Los Alamos, NM.

Brun, E., Damian, F., Diop, C.M., Dumonteil, E., Hugot, F.X., Jouanne, C., Lee, Y.K., Malvagi, F., Mazzolo, A., Petit, O., Trama, J.C., Visonneau, T., Zoia, A., 2015. TRIPOLI-4®, CEA, EDF and AREVA reference Monte Carlo code. Ann. Nucl. Energy 82, 151–160.

Hunt, J.G., Silva, F.C.A.d., Mauricio, C.L.P., Santos, D.S.d., 2004. The validation of organ dose calculations using voxel phantoms and Monte Carlo methods applied to point and water immersion sources. Radiat. Protect. Dosim. 108 (1), 85–89.

ICRP, 2007. The 2007 recommendations of the international commission on radiological protection. ICRP publication 103. Ann. ICRP 37 (2–4).

ICRP, 2008. Nuclear decay data for dosimetric calculations. ICRP Publication 107. Ann. ICRP 38 (3).

ICRP, 2009. Adult reference computational phantoms. ICRP Publication 110. Ann. ICRP 39 (2).

ICRP, 2010. Conversion coefficients for radiological protection quantities for external radiation exposures. ICRP publication 116. Ann. ICRP 40 (2–5).

ICRP, 2016. The ICRP computational framework for internal dose assessment for reference adults: specific absorbed fractions. Ann. ICRP 133 (2), 45. ICRP Publication.

Kawrakow, I., Mainegra-Hing, E., Rogers, D.W.O., Tessier, F., Walters, B.R.B., 2009. The EGSnrc Code System: Monte Carlo Simulation of Electron and Photon Transport. National Research Council of Canada (NRCC), Ottawa.

Lee, Y.-K., Hugot, F.-X., Jin, Y., 2021. New Route in TRIPOLI-4® for Radiation Dosimetry Calculations Using ICRP 110 Voxel Phantoms, ANS M&C 2021, International Conference on Mathematics and Computational Methods Applied to Nuclear Science and Engineering. American Nuclear Society, Raleigh, NC, USA.

Pelowitz, D.B.e., 2008. MCNPX User's Manual, Version 2.6.0. Los Alamos National Laboratory, Los Alamos, NM.

Seltzer, S.M., Berger, M.J., 1985. Bremsstrahlung spectra from electron interactions with screened atomic nuclei and orbital electrons. Nucl. Instrum. Methods Phys. Res., Sect. B 12, 95–134.

Seltzer, S.M., Berger, M.J., 1986. Bremsstrahlung energy spectra from electrons with kinetic energy from 1 keV to 10 GeV incident on screened nuclei and orbital electrons of neutral atoms with Z=1-100. Atomic Data Nucl. Data Tables 35, 345–418.

Sempau, J., Badal, A., Brualla, L., 2011. A PENELOPE-based system for the automated Monte Carlo simulation of clinacs and voxelized geometries—application to far-from-axis fields. Med. Phys. 38 (11), 5887–5895.

Seuntjens, J.P., Kawrakow, I., Borg, J., Hobeila, F., Rogers, D.W.O., 2002. Calculated and measured air-kerma response of ionization chambers in low and medium energy photon beams. In: Seuntjens, J.P., Mobit, P. (Eds.), Recent Developments in Accurate Radiation Dosimetry, Proc. Of an Int'l Workshop. Medical Physics Publishing, Madison, USA, pp. 69–84.

Werner, C.J., Armstrong, J., Brown, F.B., Bull, J.S., Casswell, L., Cox, L.J., Dixon, D., Forster, R.A., Goorley, J.T., Hughes, H.G., Favorite, J., Martz, R., Mashnik, S.G., Rising, M.E., Solomon, C., Sood, A., Sweezy, J.E., Zukaitis, A., Anderson, C., Elson, J. S., Durkee, J.W., Johns, R.C., McKinney, G.W., McMath, G.E., Hendricks, J.S., Pelowitz, D.B., Prael, R.E., Booth, T.E., James, M.R., Fensin, M.L., Wilcox, T.A., Kiedrowski, B.C., 2017. MCNP User's Manual - Code Version 6.2. Los Alamos National Laboratory, Los Alamos, NM.

Zankl, M., Eakins, J., Gómez Ros, J.-M., Huet, C., Jansen, J., Moraleda, M., Reichelt, U., Struelens, L., Vrba, T., 2021a. EURADOS intercomparison on the usage of the ICRP/ICRU adult reference computational phantoms. Radiat. Meas. 145, 106596.

Zankl, M., Eakins, J.S., Gómez Ros, J.-M., Huet, C., 2021b. The ICRP recommended methods of red bone marrow dosimetry. Radiat. Meas. 146, 106611.

Zankl, M., Schlattl, H., Petoussi-Henss, N., Hoeschen, C., 2012. Electron specific absorbed fractions for the adult male and female ICRP/ICRU reference computational phantoms. Phys. Med. Biol. 57, 4501–4526.